Atmos. Chem. Phys., 22, 3433–3444, 2022
https://doi.org/10.5194/acp-22-3433-2022
© Author(s) 2022. This work is distributed under
the Creative Commons Attribution 4.0 License.

Atmospheric Chemistry and Physics
Open Access
EGU



# Measurement report: Ice-nucleating particles active ≥ −15 °C in free tropospheric air over western Europe

**Franz Conen**[1], **Annika Einbock**[1], **Claudia Mignani**[1], **and Christoph Hüglin**[2]

[1]Department of Environmental Sciences, University of Basel, 4056 Basel, Switzerland
[2]Laboratory for Air Pollution/Environmental Technology, Empa, 8600 Dübendorf, Switzerland

**Correspondence:** Franz Conen (franz.conen@unibas.ch)

Received: 21 October 2021 – Discussion started: 15 November 2021
Revised: 1 February 2022 – Accepted: 13 February 2022 – Published: 15 March 2022

**Abstract.** Ice-nucleating particles (INPs) initiate ice formation in supercooled clouds, typically starting in western Europe at a few kilometres above the ground. However, little is known about the concentration and composition of INPs in the lower free troposphere (FT). Here, we analysed INPs active at −10 °C ($INP_{-10}$) and −15 °C ($INP_{-15}$) that were collected under FT conditions at the high-altitude observatory Jungfraujoch between January 2019 and March 2021. We relied on continuous radon measurements to distinguish FT conditions from those influenced by the planetary boundary layer. Median concentrations in the FT were 2.4 $INP_{-10}$ $m^{-3}$ and 9.8 $INP_{-15}$ $m^{-3}$, with a multiplicative standard deviation of 2.0 and 1.6 respectively. A majority of INPs were deactivated after exposure to 60 °C; thus, they probably originated from certain epiphytic bacteria or fungi. Subsequent heating to 95 °C deactivated another 15 % to 20 % of the initial INPs, which were likely other types of fungal INPs that might have been associated with soil organic matter or with decaying leaves. Very few $INP_{-10}$ withstood heating to 95 °C, but on average 20 % of $INP_{-15}$ in FT samples did so. This percentage doubled during Saharan dust intrusions, which had practically no influence on $INP_{-10}$. Overall, the results suggest that aerosolised epiphytic microorganisms, or parts thereof, are responsible for the majority of primary ice formation in moderately supercooled clouds above western Europe.

## 1 Introduction

The free troposphere (FT) refers to a part of the troposphere that is only occasionally in exchange with the Earth's surface, whereas the planetary boundary layer (PBL) continuously exchanges particles with surface sources and sinks. Consequently, the FT integrates particle emissions over a much larger area compared with the PBL. For example, in the PBL, a community of airborne microorganisms is mainly composed of organisms emitted from sources within a distance of several tens of kilometres around an observation point (Tignat-Perrier et al., 2019). In contrast, particle populations sampled at a high-altitude mountain station under FT conditions constitute a mixture of many sources and sinks active on a continental scale (Herrmann et al., 2015, Sun et al., 2021). A special kind of aerosol particle, so-called ice-nucleating particles (INPs), is relevant for primary ice formation in mid-level clouds (Findeisen, 1938). Ice formation in clouds above lowlands in western Europe starts at a few kilometres altitude at around −5 °C (Kanitz et al., 2011). However, FT air masses have been little explored in terms of the INPs that they carry, let alone the INPs active > −15 °C. For recent summaries of INP studies in the FT, see Lacher et al. (2018) and He et al. (2021). Under FT conditions at the high-altitude observatory Jungfraujoch (3580 m a.s.l.) in the Swiss Alps, Lacher et al. (2018) found similar concentrations of INPs active at −31 °C ($INP_{-31}$) as had been reported for the FT in other regions of the world (summarised in Table 2 and Fig. 6 in Lacher et al., 2018) as well as little seasonal variation. Later, continuous measurements by Brunner et al. (2021b) found the monthly median of $INP_{-30}$ in the FT background to peak in April and to be lowest in December.

Brunner et al. (2021a, b) found that most $INP_{-30}$ at Jungfraujoch occurred during Saharan dust intrusions, by far exceeding any background concentration. However, in the PBL and at more moderate supercooling (here, ≥ −15 °C), biological particles seemed to constitute the majority of the INP population as revealed by heat tests (Hill et al., 2016). Heat deactivates biological INPs but leaves mineral INPs largely unaffected (Hill et al., 2016). During dust events sampled in Beijing, Chen et al. (2021) found that 70 % of INPs active at ≥ −15, °C ($INP_{-15}$) were heat sensitive. Observed heat-sensitive fractions of $INP_{-15}$ in the PBL of agricultural areas in the USA (Suski et al., 2018) and in Argentina (Testa et al., 2021) were even larger (> 90 %). These findings contrast with a small biological fraction detected among ice particle residuals collected at Jungfraujoch from mixed-phase clouds and classified by physico-chemical analyses (Mertes et al., 2007) or by laser ablation mass spectrometry (Schmidt et al., 2017; Lacher et al., 2021). Not every ice particle residual has initiated as INP the formation of the ice particle it was recovered from, in particular not when it was recovered from a secondary ice particle. An ice particle residual recovered from a primary ice particle and classified by mass spectrometry as mineral dust may have been activated at moderate supercooling by a minor, ice nucleation active biological component sticking to its surface (Augustin-Bauditz et al., 2016). A heat test, which specifically targets the ice nucleation active component, would have classified the same assembly as a biological INP.

Aerosolisation of biological particles from vegetated land to the PBL is intensified during rainfall (Huffman et al. 2013; Prenni et al., 2013; Iwata et al., 2019). Subsequent transport from the PBL to the FT may happen through mixing in frontal systems, cloud convection, or by mountain venting (Henne et al., 2005). Here, we investigate whether biological INPs, as classified by heat tests, also contribute the majority of the INP population in the FT. Our objectives were to quantify INPs active at moderate supercooling in the FT and to narrow down the likely composition of these INPs and how this composition might change during Saharan dust intrusions (SDIs). We will also compare INP concentrations in the FT with those of air masses influenced by the PBL as presented in earlier studies.

## 2 Material and methods

### 2.1 Sampling and analysis

For our investigation, we relied on archived samples of particulate matter ($PM_{10}$) collected between January 2019 and March 2021 (Table A1) on quartz-fibre filters at the high-altitude observatory Jungfraujoch (07°59′02″ E, 46°32′53″ N; 3580 m a.s.l.), which is part of the Swiss national air quality monitoring network. $PM_{10}$ sampling and INP analysis at the site have been described in previous work (Conen et al., 2012). Units of air volume throughout this paper are normalised to standard pressure. Briefly, air was sampled at a rate of 720 $m^3$ $d^{-1}$ through a heated inlet, followed by a $PM_{10}$ cut-off, onto a 150 mm diameter quartz-fibre filter (Pallflex Tissuquartz 2500-UP) with a 140 mm diameter of active area. Every day at midnight a new filter was exposed to the continuous air stream for 24 h. From each selected filter, we took 72 punches with a 2 mm diameter each; all 72 punches together contained aerosol particles from a total of 10.6 $m^{-3}$. Each punch was placed into a 0.5 mL Eppendorf safe-lock tube, and 0.1 mL of ultra-pure water (Sigma-Aldrich, W4502-1L) was added. The tubes were then immersed in a cooling bath and exposed to a temperature ramp from −5 to −15 °C (0.3 °C $min^{-1}$). After each 1 °C step, the number of frozen tubes was counted by eye, and the cumulative concentration of INPs was calculated according to Vali (1971). After the first such freezing assay, the tubes were placed in a water bath at 60 °C for 10 min before the freezing assay was repeated. This was followed by a second 10 min heat treatment at 95 °C and a third freezing assay. Loss of INPs active < −10 °C due to the repeated freezing is unlikely in this study. Although Polen et al. (2016) observed some loss of INPs active > −5 °C throughout five repeated freezing assays, little had changed in INPs active < −5 °C (see Fig. 6 in Polen et al., 2016). A more extensive set of tests was conducted by Vali (2008) on a soil sample. After 55 refreezing cycles, an increasingly larger fraction of INPs had been lost above −10 °C toward the warmer end of the freezing spectrum, but the concentration of INPs active < −10 °C had remained practically the same (Fig. 1c in Vali, 2018).

Probably the largest uncertainty in these assays is related to the often small number of INPs assessed. The 68 % confidence interval ($\pm 1\sigma$) of a determined INP number concentration is roughly proportional to the square root of the INPs in an assay. In this study, an assay contained particles collected from 10.6 $m^3$ of air. Hence, a concentration of 1 INP $m^{-3}$ was represented by a total of 10 or 11 INPs in the assay and is associated with an uncertainty of around ±0.3 INP $m^{-3}$ ($\sqrt{11}/11 \times 1$ INP $m^{-3}$). Two blank (background) assays were done with punches from 5 mm wide fringes of sample filters. This part of a filter is covered by the clamp rings holding it in place during sampling. Thus, sampled air does not pass through it, and it remains clean. However, some particles may get smeared from the active filter area onto this narrow fringe during handling and transport. Consequently, these blank values are a conservative (upper) estimate of a field blank. Each of these blanks was composed of punches from four filters. Sample values were corrected for blank values by subtracting the average of both blanks, which on average was 7 % of a sample value. We calculated by difference the number concentration of heat-sensitive INPs (INPs active before any heat treatment − INPs active after 60 °C treatment) and moderately heat-tolerant INPs (INPs active after 60 °C treatment − INPs active after 95 °C treatment). What remained active after the 95 °C treatment was termed heat tolerant. In one sample (6 February 2021), the assay was

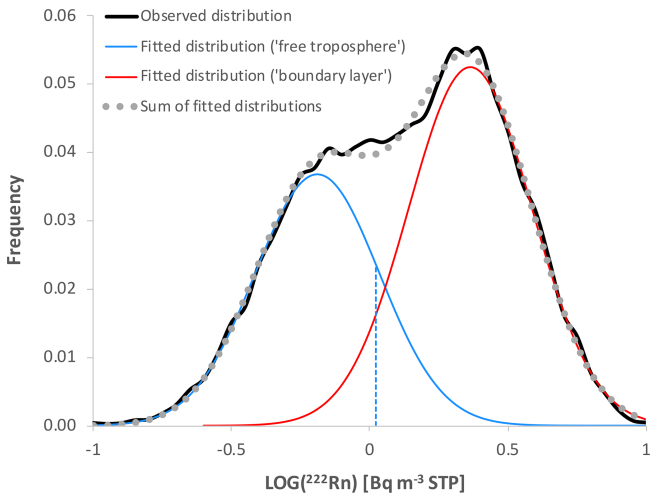


**Figure 1.** Probability density function of the log-transformed hourly mean radon concentration observed during the years from 2016 to 2020 at Jungfraujoch (black line). The sum of two fitted and weighed log-normal distributions (grey dotted line) closely matches the observed distribution. The fitted distributions most likely represent the distribution of free tropospheric air masses (blue continuous line) and that of air masses influenced by the planetary boundary layer (red line). Ninety percent of the values below the dashed vertical line belong to the fitted "free troposphere" distribution (figure adapted from Conen et al., 2021).

completely frozen at −15 °C and was repeated with smaller punches (1 mm diameter).

#### 2.1.1 Identification of free tropospheric conditions

A key issue in our study is the distinction between FT and PBL-influenced air masses. For this purpose, we routinely monitor radon ($^{222}$Rn) at Jungfraujoch with a dual-loop two-filter detector (Whittlestone and Zahorowski, 1998). Radon is emitted relatively homogenously in space and time from land surfaces. Its only sink in the atmosphere is radioactive decay. Because of its short half-life (3.82 d), the concentration difference is large between the FT and the PBL, making radon a useful tracer to discriminate between these two types of air masses (Herrmann et al., 2015; Chambers et al., 2016). The probability density function of all hourly mean radon concentrations measured over the past 5 years is well reproduced by the sum of two log-normal distributions (Fig. 1), most likely representing FT- and PBL-influenced air masses (Conen et al., 2021, Brunner et al., 2021a). Although FT conditions prevailed 41.5 % of the time, it was only on 1 in 13 d in 2019 and 2020 that such conditions applied to every hour of a full 24 h $PM_{10}$ sampling period. Here, we consider a 24 h $PM_{10}$ sampling period as representative of the FT when all 24 values of the hourly mean radon concentration during the sampling period were below 1.05 Bq m$^{-3}$. Ninety percent of all values below 1.05 Bq m$^{-3}$ belong to the distribution representing FT conditions (Fig. 1). Two-thirds of the FT samples defined that way were collected in the months of January, February, and March. We selected 28 such samples from between January 2019 and March 2021 for INP analysis, making sure to have samples from each month of the year for which they were available. In addition, from the filter archive, we selected an additional seven samples with high $PM_{10}$ loads and a yellow-brown (ochre) colour resulting from SDIs (Collaud Coen et al., 2004) .

The median radon concentration in the FT distribution is only 0.28 times that of the PBL-influenced distribution (Fig. 1); hence, PBL injections in the FT may have a median age of about 7 d. Thus, the airshed from which the INPs in FT air masses sampled at Jungfraujoch might have originated is roughly indicated by 7 d backward trajectories calculated using the HYSPLIT model (Fig. 2). One trajectory was calculated for each day, ending at 13:00 UTC at 500 m a.g.l., which is 1500 m a.s.l. for Jungfraujoch in the model surface. The model was run with the following settings: the meteorology was from the Global Data Assimilation System (GDAS; 1°, global); the vertical motion calculation method was model vertical velocity; and the location coordinates were 46°32′53″ N, 07°59′02″ E.

## 3 Results and discussion

### 3.1 Concentration and likely composition of ice-nucleating particles in free tropospheric air

The observed range of the INP concentration in FT air masses was 1.0 to 5.6 m$^{-3}$ for INPs active at −10 °C ($INP_{-10}$) and 4.1 to 16.3 m$^{-3}$ for INPs active at −15 °C ($INP_{-15}$). These values are within the lower range of INP concentrations observed in other contexts (Petters and Wright, 2015). The INPs sampled at Jungfraujoch under FT conditions likely originated from the northern part of western Europe and from the North Atlantic (Fig. 2). The latter influence was probably minor. McCluskey et al. (2018) found a mean of 1.1 $INP_{-15}$ m$^{-3}$ in pristine marine air masses arriving at the west coast of Ireland, which was 1/10 of the median that we found at Jungfraujoch. A majority of $INP_{-10}$ (83 %) and $INP_{-15}$ (57 %) species in the FT were heat sensitive and lost their activity after exposure to a temperature of 60 °C (Table 1; for INPs active at other temperatures between −8 and −15 °C, see Table A3). Possible contributors to this category include the bacteria *Erwinia herbicola* (Phelps et al., 1986) and *Pseudomonas* sp. (Pouleur et al., 1992) as well as heat-sensitive spores of several fungal species (Table 2). These microorganisms live on plant surfaces from where they, or parts of them, are emitted to the atmosphere (Lindow et al., 1978; Lindemann et al., 1982; Hirno and Upper, 2000; Huffman et al., 2013). Further potential sources include other fungi, such as *Fusarium graminearum* (Vujanovic et al., 2012; Keller et al., 2014) and *Puccinia* sp. (Morris et al., 2013). However, we do not know whether these species lose their ice nucleation activity at 60 °C or be-

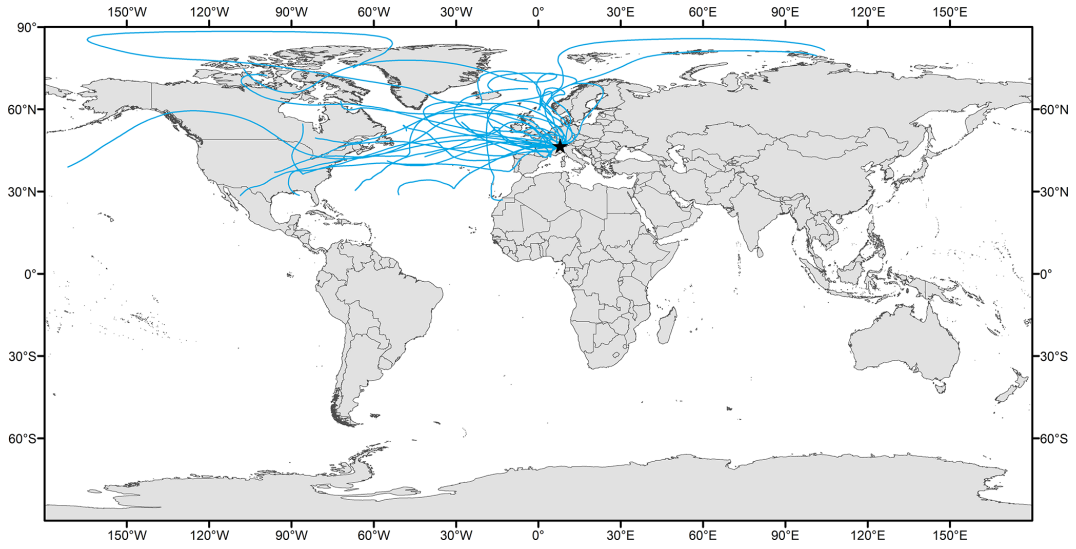


**Figure 2.** Ensemble of 7 d backward trajectories ending at Jungfraujoch at noon local time on days for which we analysed INPs under free tropospheric conditions. The trajectories were calculated using the HYSPLIT model (NOAA Air Resources Laboratory; https://www.ready.noaa.gov/HYSPLIT.php (last access: 30 July 2021).

**Table 1.** The INP concentration found in the free troposphere (FT) and during Saharan dust intrusions (SDIs), categorised according to heat sensitivity. The median and multiplicative standard deviation are shown. Use of the multiplicative standard deviation ($s^*$) is appropriate because multiplicative processes determine the concentration of biological particles in the atmosphere (Limpert et al., 2001, 2008). It was estimated from the upper (Q3) and lower (Q1) quartiles of a distribution: $s^* = (Q3/Q1)^{0.741}$ (Limpert et al., 2001). It was not estimated when the lower quartile was below the detection limit ($< 0.095\,\mathrm{INP\,m^{-3}}$). INPs were designated as heat sensitive if they had lost their activity after exposure to 60 °C; INPs were termed moderately heat tolerant if they had retained their activity after exposure to 60 °C but had lost it after exposure to 95 °C; and heat-tolerant INPs were those that were still active after both heat treatments.

| Category | $INP_{-10}$ ($m^{-3}$) | | $INP_{-15}$ ($m^{-3}$) | |
|---|---|---|---|---|
| | $FT_{(n=28)}$ | $SDI_{(n=6)}$ | $FT_{(n=28)}$ | $SDI_{(n=6)}$ |
| All | $2.4_{2.0}$ | $2.4_{1.5}$ | $9.8_{1.6}$ | $20.0_{1.7}$ |
| Heat sensitive | $2.0_{1.8}$ | $1.9_{1.6}$ | $5.6_{1.5}$ | $9.2_{2.1}$ |
| Moderately heat tolerant | $0.4_{1.9}$ | $0.2_{\text{n.d.}}$ | $1.5_{2.8}$ | $3.5_{2.8}$ |
| Heat tolerant | $0.0_{\text{n.d.}}$ | $0.1_{2.8}$ | s $1.6_{1.6}$ | $6.2_{1.5}$ |

n.d. = not determinable.

tween 60 and 95 °C, as heat stress tests were only done at around 95 °C, which is why they are not included in Table 2.

Between 15 % and 20 % of the INPs that we found in the FT were moderately heat tolerant (deactivated between 60 and 95 °C). This deactivation temperature matches the profile of *Mortierella alpina*, a saprophytic fungus associated with decaying leaf litter (Vasebi et al., 2019) and with soil particles (Fröhlich-Nowoisky et al., 2015; Conen and Yakutin, 2018). Other potential sources of moderately heat-tolerant INPs include fungal symbionts in lichen (Kieft, 1988), *Fusarium avenaceum* (Pouleur et al., 1992), and the other above-mentioned fungi for which the deactivation temperature is not clearly defined. The sum of heat-sensitive and moderately heat-sensitive $INP_{-15}$ in a FT sample was on average 80 % (SD = 9 %) of its total $INP_{-15}$ content, which was slightly smaller than the combined fractions of fungal and bacterial $INP_{-15}$ (92 %) estimated in a case study over Amazonia (Patade et al., 2021).

Heat-tolerant INPs (not deactivated at 95 °C) constituted a negligibly small fraction of all $INP_{-10}$, but they contributed as much as the moderately heat-tolerant INPs to $INP_{-15}$. The fraction of heat-tolerant $INP_{-15}$ should substantially increase during SDIs if mineral dust, in particular K-feldspar, is their main component (Vergara-Temprado et al., 2017), which is an issue addressed in the next section.

### 3.2 The effect of Saharan dust intrusions

Mineral dust has by far the largest contribution to INPs activated at around −30 °C at Jungfraujoch (Larcher et al., 2018, 2021; Brunner et al., 2021a, b). Most INPs in airborne min-

**Table 2.** Reported heat sensitivity of INPs active at moderate supercooling. Indicated is the temperature range in which at least 90 % of a specific type of INPs active ≥ 15 °C was found to be deactivated, although a smaller fraction of the same INPs may already have been deactivated at a lower temperature. For example, soil particles analysed by Conen and Yakutin (2018) had lost half of their $INP_{-10}$ after exposure to 60 °C but more than 98 % after exposure to 95 °C. These particles are assigned a deactivation temperature between 60 and 95 °C. Note that studies where INPs were found to be deactivated after a single heat treatment ∼ 95 °C are not listed because deactivation might already have happened < 60 °C.

| Type | Deactivation temperature | | | Reference |
|---|---|---|---|---|
| | < 60 °C | 60–95 °C | > 95 °C | |
| Bacteria | *Erwinia herbicola* | | | Phelps et al. (1986) |
| | *Pseudomonas* sp. | | | Pouleur et al. (1992) |
| | | | *Lysinibacillus* sp. | Failor et al. (2017) |
| Fungi | *Acremonium implicatum* | | | Pummer et al. (2015) |
| | *Isaria farinosa* | | | Pummer et al. (2015) |
| | *Fusarium acuminatum* | | | Kunert et al. (2019) |
| | *Fusarium langsethiae* | | | Kunert et al. (2019) |
| | *Fusarium armeniacum* | | | Kunert et al. (2019) |
| | | Fungal symbiont in lichen | | Kieft (1988) |
| | | *Mortierella alpina* | | Fröhlich-Nowoisky et al. (2015) |
| | | *Fusarium avenaceum* | | Pouleur et al. (1992) |
| Others | | | | |
| Mixed | | Leaf-derived ice nuclei | | Schnell and Vali (1973) |
| | | Soil particles | | Hill et al. (2016) |
| | | Soil particles | | Conen and Yakutin (2018) |
| Organic | | | Pollen | Diehl et al. (2002), Pummer et al. (2012) |
| | | | Lignin | Bogler and Borduas-Dedekind (2020) |
| Mineral | | | K-feldspars | Daily et al. (2021) |
| | | | Montmorillonite | Conen et al. (2011) |
| | | | Illite | O'Sullivan et al. (2015) |
| | | | Kaolinite | Daily et al. (2021) |

eral dust are probably K-feldspars, some of which are already activated at temperatures above −10 °C (Boose et al., 2016; Harrison et al., 2019). Here, we analysed seven samples collected during SDIs (Appendix Table A1), but we excluded one sample from further analysis (6 February 2021) in which INPs had substantially increased at −15 °C after each heat treatment. A similar reaction to heating was previously observed by Boose et al. (2019), and it was explained by the removal of secondary organic coatings that had masked ice nucleation active sites before the heat treatment. In the remaining six samples, the median $PM_{10}$ concentration was 19 times as large as in FT samples. Surprisingly, the median concentration of heat-tolerant $INP_{-15}$ during SDIs was larger by only a factor of 4 compared with the FT (Table 1). Hence, mineral dust cannot be the main heat-tolerant $INP_{-15}$ in the FT, as SDIs, which consist mainly of mineral dust, would have led to an increase in the heat-tolerant fraction of $INP_{-15}$ that is roughly proportional to the increase in dust load. This assumption is based on the finding that a large fraction of the particle volume (i.e. mass) during an SDI event at Jungfraujoch falls into the size range of particles > 0.5 µm in optical diameter (Schwikowski et al., 1995), which is a good predictor of atmospheric $INP_{-15}$ (DeMott et al., 2010; Mignani et al., 2021). As we found no peak in heat-tolerant $INP_{-15}$ during the main pollen season in spring, pollen and pollen fragments (Diehl et al., 2002; Pummer et al., 2012) are also an unlikely source of these particles. (Note that Burkart et al. (2021) recently found convincing evidence that ice nucleation activity in birch pollen is related to a protein. Therefore, it probably is also heat sensitive, contrarily to earlier conclusions.) More likely candidates of the heat-tolerant fraction in the FT include soil organic material, stabilised through bonding to minerals surfaces against deactivation by heat (Perkins et al., 2020), or lignin, not necessarily bound to mineral surfaces (Bogler and Borduas-Dedekind, 2020). Such organic compounds are more abundant in fertile soils in the mid-latitudes compared with desert soils and could explain the comparatively small effect of SDIs on heat-tolerant $INP_{-15}$ observed at Jungfraujoch.

Further, the medians of heat-sensitive and of moderately heat-tolerant $INP_{-15}$ were a factor of 1.6 and 2.3 larger during SDIs respectively (Table 1). Their increase may be due to

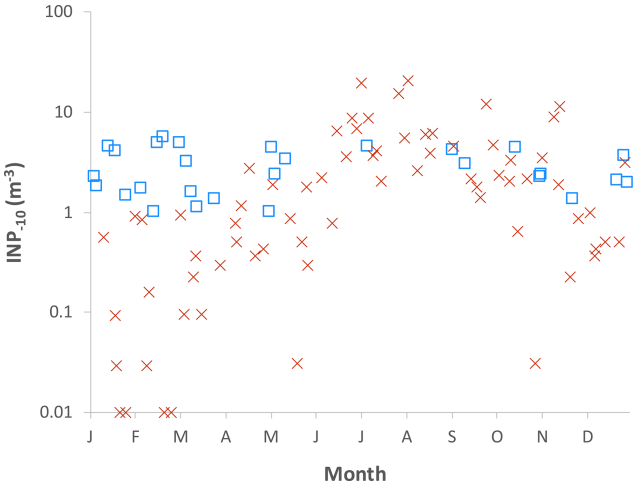


**Figure 3.** The concentration of $INP_{-10}$ when free tropospheric conditions prevailed at Jungfraujoch throughout a full day (open squares) and for days not selected for this criterion (crosses); data are from Conen et al. (2015) (see Table A2).

a concurrent influence of the PBL with all SDIs, as suggested by enhanced radon concentrations (Table A1). Overall, SDIs and the associated PBL influence doubled the median concentration of $INP_{-15}$ and doubled the average fraction of heat-tolerant $INP_{-15}$ in a sample but had no discernable effect on the median concentration of $INP_{-10}$ (Table 1).

### 3.3 Comparison with other studies in the Swiss Alps

Mignani et al. (2021) made a large number of impinger-based $INP_{-15}$ measurements ($n = 124$, each integrating over 20 min) in February and March 2019 at Weissfluhjoch, a mountain station 145 km east of Jungfraujoch and at a 909 m lower elevation (2671 m a.s.l.). This station was increasingly influenced by air from the PBL throughout the day (Wieder et al., 2021). The median of all observations, excluding those influenced by SDIs ($n = 11$), was 15.5 $m^{-3}$ ($s^* = 4.0\,m^{-3}$). This value is about a factor of 2 larger than the median of the four FT samples collected at Jungfraujoch during the same months, February and March 2019 (8.9 $m^{-3}$ with a range of 5.5 to 13.0 $m^{-3}$). A factor of 2 decrease with an increase of 1000 m in altitude has already been observed for $INP_{-8}$ in Switzerland (Conen et al., 2017). Similar to the present study, SDIs at Weissfluhjoch enhanced the median $INP_{-15}$ concentration by much less than the concurrent increase in particle number concentration.

A surprising feature of $INP_{-10}$ in FT samples is their narrow distribution (1.0 to 5.6 $m^{-3}$) throughout the year (Fig. 3), which is in contrast to what we had found earlier at Jungfraujoch for filters not selected for FT conditions that covered a range of 3 orders of magnitude (Conen et al., 2015). Those filters were sampled between June 2012 and May 2013 and analysed using the same method described in this study, although without the heat treatments. Generally, the influence of the PBL on Jungfraujoch is largest in summer and smallest in winter (Collaud Coen et al., 2011; Griffith et al., 2014). Hence, if samples are not explicitly selected for FT conditions, the majority of them will have at least some PBL influence, in particular during summer (Brunner et al., 2021b). Therefore, the concentration of $INP_{-10}$ on filters not selected for FT conditions occasionally exceeded that of filters selected for FT conditions, in particular during summer (Fig. 3). However, the opposite was true for winter. Especially during January and February, the concentration of $INP_{-10}$ was 1 or 2 orders of magnitude smaller in the randomly selected samples from the year 2013 compared with the FT samples for the years 2019, 2020, and 2021. A plausible explanation for this difference could be that a substantially larger fraction of $INP_{-10}$ had been activated and deposited before reaching Jungfraujoch in 2013 compared with the later years. Indeed, mean air temperature during sampling in January and February 2013 at Jungfraujoch was −16.2 °C (SD 5.3 °C), which is 6.4 °C colder than during sampling in January and February 2019, 2020, and 2021 (−9.8 °C; SD 4.6 °C). However, high relative humidity and low temperature does not always result in a particularly low number concentration of $INP_{-10}$ being recorded at Jungfraujoch. On 14 March 2021 an exceptionally strong storm from the north-west passed Jungfraujoch, with gusts of up to 122 km $h^{-1}$ and a mean daily wind speed of 51.5 km $h^{-1}$. Daily mean values of relative humidity and temperature were 98 % and −18.8 °C respectively. Nevertheless, we found a non-negligible concentration of $INP_{-10}$ (0.7 $m^{-3}$) on the $PM_{10}$ filter from that day. The updraught velocity at Jungfraujoch can reach a 6 min mean value of 8 m $s^{-1}$ under north-westerly wind conditions (Hammer et al., 2014). An $INP_{-10}$ activated 1350 m below Jungfraujoch at −10 °C would grow for about 3 min ((18.8–10.0 °C)/6.5 °C $km^{-1}$/8 m $s^{-1}$ = 169 s) into a crystal with a fall velocity of 5 cm $s^{-1}$ (Fukuta and Takahashi, 1999). As such, it could still enter the heated inlet of the sampler, which takes in droplets up to a size of about 40 µm (Weingartner et al., 1999); evaporate; and let the $INP_{-10}$ pass the $PM_{10}$ cut-off and be collected on the filter. At a lower wind speed, the growth time increases, and activated $INP_{-10}$ species are more likely to either settle or become too large to enter the heated inlet, eventually leading to very low concentrations; this might explain our earlier observations in 2013. In an increasingly warmer climate, seasonality in the sink term of INPs active under moderately supercooled conditions above the Alps may fade.

In summary, the results of this study suggest that epiphytic microorganisms contribute the majority of INPs to ice formation in moderately supercooled clouds above the northern part of western Europe, whereas the impact of Saharan dust is negligible at −10 °C and still limited at −15 °C.

## Appendix A

**Table A1.** Number concentration of ice-nucleating particles active at −10 °C ($INP_{-10}$) and at −15 °C ($INP_{-15}$) at Jungfraujoch, determined for free tropospheric conditions and during Saharan dust intrusions. The same sample material was analysed three times. A first freezing assay was followed by a heat treatment (10 min at 60 °C) and second freezing assay, followed by a second heat treatment (10 min at 95 °C) and a third freezing assay. All steps were carried out in an uninterrupted operation. Blank values were subtracted from raw measured values. Three categories of INPs were derived by calculating the difference between the INP number concentration before and after each heat treatment, resulting in negative values if the INP concentration had increased after a heat treatment. Meteorological data are from MeteoSwiss, and $PM_{10}$ data are from the Swiss National Air Pollution Monitoring Network (NABEL).

| Date (dd.mm.yyyy) | $INP_{-10}$ ($m^{-3}$) | | | $INP_{-15}$ ($m^{-3}$) | | | $T_{mean}$ | Fraction of hours with RH > 95 % | Radon | | | $PM_{10}$ |
|---|---|---|---|---|---|---|---|---|---|---|---|---|
| | Deactivation temperature (°C) | | | Deactivation temperature (°C) | | | | | Min | Max | Mean | |
| | < 60 | 60–95 | > 95 | < 60 | 60–95 | > 95 | (°C) | | ($Bq\,m^{-3}$) | | | ($\mu g\,m^{-3}$) |
| Free tropospheric conditions | | | | | | | | | | | | |
| 06.01.2019 | 1.6 | 0.3 | 0.0 | 5.1 | 0.7 | 1.1 | −13.1 | 0.00 | 0.32 | 0.48 | 0.39 | 0.5 |
| 26.01.2019 | 1.1 | 0.3 | 0.1 | 3.8 | 1.5 | 1.6 | −11.1 | 0.00 | 0.20 | 0.40 | 0.29 | 0.7 |
| 05.02.2019 | 1.5 | 0.2 | 0.0 | 4.3 | 0.1 | 0.7 | −9.6 | 0.00 | 0.30 | 0.62 | 0.46 | 0.8 |
| 03.03.2019 | 3.8 | 1.2 | 0.1 | 10.4 | 1.7 | 1.3 | −8.4 | 0.04 | 0.30 | 0.82 | 0.54 | 0.9 |
| 08.03.2019 | 2.3 | 0.8 | 0.1 | 6.6 | 2.6 | 3.6 | −13.8 | 0.04 | 0.45 | 0.86 | 0.66 | 0.8 |
| 27.03.2019 | 1.2 | 0.2 | 0.0 | 3.9 | −0.2 | 1.3 | −8.7 | 0.00 | 0.22 | 0.48 | 0.34 | 1.3 |
| 07.05.2019 | 2.2 | 0.1 | 0.1 | 6.3 | 1.8 | 2.0 | −7.7 | 0.00 | 0.37 | 0.92 | 0.58 | 1.9 |
| 14.05.2019 | 2.9 | 0.3 | 0.2 | 7.0 | 1.8 | 5.6 | −7 | 0.00 | 0.29 | 1.01 | 0.51 | 2.3 |
| 03.09.2019 | 2.6 | 1.6 | 0.0 | 5.6 | 2.9 | 1.6 | 1.3 | 0.00 | 0.35 | 0.75 | 0.48 | 1.4 |
| 12.09.2019 | 1.7 | 1.4 | 0.0 | 3.1 | 3.6 | 4.3 | 1.2 | 0.13 | 0.21 | 0.99 | 0.48 | 1.1 |
| 16.10.2019 | 3.3 | 1.1 | 0.0 | 5.3 | 2.2 | 2.1 | −4.9 | 0.13 | 0.43 | 0.69 | 0.56 | 0.6 |
| 28.12.2019 | 3.3 | 0.3 | 0.1 | 7.3 | 1.3 | 2.0 | −7 | 0.00 | 0.43 | 0.94 | 0.64 | 0.7 |
| 30.12.2019 | 1.6 | 0.4 | 0.0 | 2.9 | 0.1 | 1.1 | −2.4 | 0.00 | 0.38 | 1.01 | 0.68 | 0.4 |
| 05.01.2020 | 1.7 | 0.5 | 0.1 | 7.5 | 0.1 | 1.2 | −7.5 | 0.00 | 0.26 | 0.78 | 0.43 | 0.5 |
| 14.01.2020 | 4.0 | 0.6 | 0.0 | 10.5 | 1.4 | 1.0 | −6.1 | 0.00 | 0.54 | 0.84 | 0.68 | 1.1 |
| 16.02.2020 | 4.2 | 0.6 | 0.2 | 8.9 | 1.3 | 2.0 | −0.9 | 0.00 | 0.23 | 0.66 | 0.49 | 0.8 |
| 20.02.2020 | 4.9 | 0.7 | 0.0 | 11.4 | 1.6 | 3.3 | −10.1 | 0.00 | 0.19 | 0.51 | 0.34 | 1.7 |
| 10.03.2020 | 1.4 | 0.1 | 0.1 | 7.4 | 0.3 | 1.4 | −8.4 | 0.08 | 0.16 | 0.96 | 0.45 | 2.6 |
| 02.05.2020 | 0.7 | 0.3 | 0.0 | 1.9 | 1.6 | 1.0 | −8.8 | 0.00 | 0.48 | 1.04 | 0.79 | 0.5 |
| 03.05.2020 | 3.9 | 0.5 | 0.0 | 9.8 | 3.0 | 3.4 | −9.2 | 0.04 | 0.22 | 0.88 | 0.50 | 0.9 |
| 07.07.2020 | 2.4 | 2.2 | 0.1 | 3.9 | 6.1 | 6.3 | 0.3 | 0.00 | 0.50 | 1.00 | 0.73 | 1.3 |
| 31.10.2020 | 1.8 | 0.3 | 0.2 | 4.9 | 2.5 | 1.8 | −0.9 | 0.00 | 0.48 | 0.98 | 0.66 | 0.7 |
| 01.11.2020 | 1.7 | 0.5 | 0.2 | 6.8 | 2.6 | 0.6 | −1.3 | 0.42 | 0.26 | 0.64 | 0.46 | 0.6 |
| 22.11.2020 | 0.9 | 0.5 | 0.0 | 4.4 | 0.9 | 0.7 | −2.3 | 0.00 | 0.31 | 0.96 | 0.56 | 0.7 |
| 22.12.2020 | 2.2 | −0.1 | 0.0 | 5.5 | 0.1 | 1.8 | −7 | 0.00 | 0.15 | 0.35 | 0.22 | 0.4 |
| 19.01.2021 | 4.1 | 0.0 | 0.0 | 12.8 | −0.1 | 1.6 | −13 | 0.00 | 0.34 | 0.64 | 0.49 | 1.6 |
| 14.02.2021 | 0.7 | 0.2 | 0.1 | 5.7 | 0.9 | 0.9 | −17 | 0.00 | 0.30 | 0.62 | 0.40 | 0.5 |
| 14.03.2021 | 0.5 | 0.5 | 0.1 | 1.5 | 2.3 | 0.4 | −18.8 | 0.83 | 0.57 | 0.90 | 0.75 | 1.7 |
| Saharan dust intrusions | | | | | | | | | | | | |
| 25.01.2020 | 2.4 | −0.1 | 0.5 | 5.7 | 1.0 | 2.1 | −11.0 | 0.00 | 2.10 | 4.99 | 3.01 | 20.8 |
| 03.02.2020 | 1.5 | 0.9 | 0.1 | 4.5 | 1.9 | 5.1 | −5.9 | 0.00 | 1.17 | 2.31 | 1.68 | 8.7 |
| 21.03.2020 | 4.8 | 0.3 | 0.1 | 13.9 | 5.1 | 9.4 | −8.8 | 0.00 | 1.24 | 5.03 | 2.71 | 16.5 |
| 22.03.2020 | 1.2 | 0.2 | 0.0 | 13.0 | 9.9 | 5.6 | −9.2 | 0.00 | 0.46 | 5.14 | 3.60 | 9.6 |
| 08.11.2020 | 2.3 | −0.1 | 0.0 | 12.7 | 1.5 | 6.8 | −4.3 | 0.00 | 1.37 | 4.06 | 2.36 | 13.8 |
| 06.02.2021 | 1.5 | 1.2 | 0.4 | −25.1 | −37.8 | 116.0 | −7.2 | 0.00 | 1.15 | 3.91 | 2.47 | 147.1 |
| 03.03.2021 | 0.4 | 0.5 | 0.1 | −0.2 | 6.8 | 12.4 | −7.1 | 0.00 | 1.25 | 2.40 | 1.58 | 61.5 |

**Table A2.** Number concentration of ice-nucleating particles active at −10 °C ($INP_{-10}$) at Jungfraujoch, determined from randomly selected $PM_{10}$ filter samples. Each sample was collected throughout a full calender day, for which the local mean air temperature and the fraction of hours with relative humidity above 95 % are shown. The INP data are from the study by Conen et al. (2015), and meteorological data are from MeteoSwiss. Assays of INPs that showed no freezing at all at −10 °C were set to a value of 0.01 $INP_{-10}$ $m^{-3}$ to be displayable on the log scale in Fig. 2.

| Date (dd.mm.yyyy) | $INP_{-10}$ ($m^{-3}$) | $T_{mean}$ (°C) | Fraction of hours with RH > 95 % | Date (dd.mm.yyyy) | $INP_{-10}$ ($m^{-3}$) | $T_{mean}$ (°C) | Fraction of hours with RH > 95 % |
|---|---|---|---|---|---|---|---|
| 06.06.2012 | 2.23 | −1.7 | 0.17 | 04.12.2012 | 1.00 | −16.6 | 0.08 |
| 13.06.2012 | 0.78 | −8.1 | 0.54 | 07.12.2012 | 0.36 | −18.1 | 0.00 |
| 16.06.2012 | 6.43 | 2.2 | 0.00 | 08.12.2012 | 0.43 | −21.1 | 0.00 |
| 23.06.2012 | 3.61 | 1.2 | 0.00 | 14.12.2012 | 0.50 | −9.9 | 0.00 |
| 27.06.2012 | 8.78 | 1.7 | 0.17 | 24.12.2012 | 0.50 | −3.7 | 0.00 |
| 30.06.2012 | 6.94 | 4.4 | 0.08 | 28.12.2012 | 3.19 | −13.7 | 0.42 |
| 03.07.2012 | 19.50 | 1.7 | 0.25 | 01.01.2013 | 0.71 | −10.7 | 0.21 |
| 08.07.2012 | 8.78 | 0.7 | 0.08 | 11.01.2013 | 0.57 | −16.2 | 0.04 |
| 11.07.2012 | 3.73 | −1.1 | 0.04 | 19.01.2013 | 0.09 | −9.5 | 0.04 |
| 13.07.2012 | 4.07 | −0.9 | 0.17 | 20.01.2013 | 0.03 | −11.9 | 0.13 |
| 16.07.2012 | 2.05 | −5 | 0.25 | 22.01.2013 | 0.01 | −18.8 | 0.00 |
| 28.07.2012 | 15.38 | 2 | 0.17 | 26.01.2013 | 0.01 | −14.2 | 0.00 |
| 01.08.2012 | 5.50 | 3.2 | 0.17 | 01.02.2013 | 0.92 | −9.5 | 0.54 |
| 03.08.2012 | 20.74 | 1.8 | 0.00 | 06.02.2013 | 0.85 | −21.3 | 0.96 |
| 10.08.2012 | 2.60 | −0.8 | 0.17 | 09.02.2013 | 0.03 | −26.8 | 0.54 |
| 15.08.2012 | 5.95 | 3 | 0.17 | 11.02.2013 | 0.16 | −17.4 | 0.00 |
| 18.08.2012 | 3.95 | 7.4 | 0.00 | 21.02.2013 | 0.01 | −20 | 0.13 |
| 20.08.2012 | 6.10 | 5.8 | 0.13 | 26.02.2013 | 0.01 | −18 | 0.00 |
| 03.09.2012 | 4.55 | −0.9 | 0.21 | 04.03.2013 | 0.93 | −10.6 | 0.00 |
| 15.09.2012 | 2.14 | 0.6 | 0.00 | 06.03.2013 | 0.10 | −10.8 | 0.25 |
| 19.09.2012 | 1.80 | −7 | 0.75 | 13.03.2013 | 0.23 | −15.5 | 0.00 |
| 21.09.2012 | 1.39 | −0.9 | 0.04 | 14.03.2013 | 0.36 | −25.4 | 1.00 |
| 25.09.2012 | 12.03 | −3.9 | 0.13 | 18.03.2013 | 0.10 | −16.3 | 0.00 |
| 30.09.2012 | 4.68 | −2.9 | 0.79 | 31.03.2013 | 0.30 | −17.9 | 0.00 |
| 04.10.2012 | 2.32 | −4.4 | 0.29 | 10.04.2013 | 0.78 | −11.8 | 0.00 |
| 11.10.2012 | 2.05 | −4.3 | 0.04 | 11.04.2013 | 0.50 | −6.3 | 0.00 |
| 12.10.2012 | 3.29 | −6.1 | 0.29 | 14.04.2013 | 1.16 | −2.3 | 0.00 |
| 16.10.2012 | 0.64 | −8 | 0.00 | 19.04.2013 | 2.79 | −7.6 | 0.46 |
| 23.10.2012 | 2.14 | 1.8 | 0.00 | 23.04.2013 | 0.36 | −4.5 | 0.00 |
| 28.10.2012 | 0.03 | −16.5 | 0.00 | 29.04.2013 | 0.43 | −4.1 | 0.92 |
| 02.11.2012 | 3.51 | −10.6 | 0.00 | 05.05.2013 | 1.88 | −5.9 | 0.00 |
| 10.11.2012 | 9.02 | −7.1 | 0.58 | 17.05.2013 | 0.86 | −5.2 | 0.50 |
| 13.11.2012 | 1.88 | −4.3 | 0.00 | 22.05.2013 | 0.03 | −9.1 | 0.00 |
| 14.11.2012 | 11.31 | −2 | 0.00 | 25.05.2013 | 0.50 | −15.5 | 0.67 |
| 21.11.2012 | 0.23 | −5.8 | 0.00 | 28.05.2013 | 1.80 | −7 | 0.63 |
| 26.11.2012 | 0.86 | −6.9 | 0.63 | 29.05.2013 | 0.30 | −12.4 | 0.33 |

**Table A3.** Median number concentration of ice-nucleating particles active between −8 and −15 °C at Jungfraujoch, determined for free tropospheric conditions and during Saharan dust intrusions, and the average of two assays with blank filter material. The blank values have been subtracted from the sample values before calculating the medians shown in the table.

| Temperature (°C) | −8 | −9 | −10 | −11 | −12 | −13 | −14 | −15 |
|---|---|---|---|---|---|---|---|---|
| Category | INPs in the free troposphere ($m^{-3}$) | | | | | | | |
| All | 0.8 | 1.7 | 2.4 | 3.4 | 4.4 | 6.0 | 8.7 | 9.8 |
| Heat sensitive | 0.6 | 1.4 | 2.0 | 2.5 | 3.4 | 4.1 | 4.9 | 5.6 |
| Moderately heat tolerant | 0.3 | 0.3 | 0.4 | 0.5 | 0.6 | 0.9 | 1.2 | 1.5 |
| Heat tolerant | 0.0 | 0.0 | 0.0 | 0.2 | 0.3 | 0.5 | 0.9 | 1.6 |
| Category | INPs in Saharan dust intrusions ($m^{-3}$) | | | | | | | |
| All | 0.6 | 1.3 | 2.4 | 3.2 | 5.1 | 7.8 | 13.4 | 20.0 |
| Heat sensitive | 0.5 | 1.0 | 1.9 | 2.7 | 4.5 | 5.1 | 6.9 | 9.2 |
| Moderately heat tolerant | 0.3 | 0.2 | 0.2 | 0.2 | 0.7 | 1.0 | 1.9 | 3.5 |
| Heat tolerant | 0.0 | 0.0 | 0.1 | 0.3 | 0.5 | 1.1 | 3.3 | 6.2 |
| Category | INPs in blank filter material ($m^{-3}$) | | | | | | | |
| All | 0.0 | 0.0 | 0.1 | 0.1 | 0.2 | 0.3 | 0.4 | 0.6 |
| Heat sensitive | 0.0 | 0.0 | 0.0 | 0.0 | 0.0 | 0.2 | 0.2 | 0.2 |
| Moderately heat tolerant | 0.0 | 0.0 | 0.1 | 0.1 | 0.1 | 0.0 | 0.0 | 0.1 |
| Heat tolerant | 0.0 | 0.0 | 0.0 | 0.0 | 0.0 | 0.1 | 0.1 | 0.4 |

**Data availability.** All data used in this paper are given in Tables A1, A2, and A3 in the Appendix.

**Author contributions.** FC and CM conceived the study. CH organised the particle collection and provided the samples, and AE carried out the freezing assays. FC prepared the paper with contribution from all co-authors.

**Competing interests.** The contact author has declared that neither they nor their co-authors have any competing interests.

**Disclaimer.** Publisher's note: Copernicus Publications remains neutral with regard to jurisdictional claims in published maps and institutional affiliations.

**Acknowledgements.** We thank the International Foundation of the High Altitude Research Stations Jungfraujoch and Gornergrat (HFSJG), 3012 Bern, Switzerland, for making it possible for us to work and to operate instruments at the high-altitude observatory Jungfraujoch. We thank Claudia Zellweger and Stefan Reimann at Empa for helping us with the selection of $PM_{10}$ filter samples and for generously sending sections of them to Basel. We are grateful to Alastair Williams and his group at Australian Nuclear Science and Technology Organisation (ANSTO) for the ongoing collaboration as the supplier and supporter of the radon detection system. The radon observations are supported by the Swiss National Science Foundation (SNSF) as a contribution to the pan-European Integrated Carbon Observation System (ICOS; https://www.icos-ri.eu, last access: 2 August 2021). The authors acknowledge MeteoSwiss, for the uncomplicated provision of meteorological data through its data portal IDAweb, and the Air Resources Laboratory at NOAA, for providing access to its HYSPLIT model.

**Financial support.** This study was done with in-house means. We have not received funding specifically dedicated to this study. The support from SNSF as a contribution to ICOS, as mentioned in the acknowledgements, satisfies the demands ICOS makes to users of its open-access data.

**Review statement.** This paper was edited by Allan Bertram and reviewed by two anonymous referees.

## References


Augustin-Bauditz, S., Wex, H., Denjean, C., Hartmann, S., Schneider, J., Schmidt, S., Ebert, M., and Stratmann, F.: Laboratory-generated mixtures of mineral dust particles with biological substances: characterization of the particle mixing state and immersion freezing behavior, Atmos. Chem. Phys., 16, 5531–5543, https://doi.org/10.5194/acp-16-5531-2016, 2016.

Bogler, S. and Borduas-Dedekind, N.: Lignin's ability to nucleate ice via immersion freezing and its stability towards physicochemical treatments and atmospheric processing, Atmos. Chem. Phys., 20, 14509–14522, https://doi.org/10.5194/acp-20-14509-2020, 2020.

Boose, Y., Welti, A., Atkinson, J., Ramelli, F., Danielczok, A., Bingemer, H. G., Plötze, M., Sierau, B., Kanji, Z. A., and Lohmann, U.: Heterogeneous ice nucleation on dust particles sourced from nine deserts worldwide – Part 1: Immersion freezing, Atmos. Chem. Phys., 16, 15075–15095, https://doi.org/10.5194/acp-16-15075-2016, 2016.

Boose, Y., Baloh, P., Plötze, M., Ofner, J., Grothe, H., Sierau, B., Lohmann, U., and Kanji, Z. A.: Heterogeneous ice nucleation on dust particles sourced from nine deserts worldwide – Part 2: Deposition nucleation and condensation freezing, Atmos. Chem. Phys., 19, 1059–1076, https://doi.org/10.5194/acp-19-1059-2019, 2019.

Brunner, C., Brem, B. T., Collaud Coen, M., Conen, F., Hervo, M., Henne, S., Steinbacher, M., Gysel-Beer, M., and Kanji, Z. A.: The contribution of Saharan dust to the ice-nucleating particle concentrations at the High Altitude Station Jungfraujoch (3580 m a.s.l.), Switzerland, Atmos. Chem. Phys., 21, 18029–18053, https://doi.org/10.5194/acp-21-18029-2021, 2021a.

Brunner, C., Brem, B. T., Collaud Coen, M., Conen, F., Steinbacher, M., Gysel-Beer, M., and Kanji, Z. A.: The diurnal and seasonal variability of ice nucleating particles at the High Altitude Station Jungfraujoch (3580 m a.s.l.), Switzerland, Atmos. Chem. Phys. Discuss. [preprint], https://doi.org/10.5194/acp-2021-710, in review, 2021b.

Burkart, J., Gratzl, J., Seifried, T. M., Bieber, P., and Grothe, H.: Isolation of subpollen particles (SPPs) of birch: SPPs are potential carriers of ice nucleating macromolecules, Biogeosciences, 18, 5751–5765, https://doi.org/10.5194/bg-18-5751-2021, 2021.

Chambers, S. D., Williams, A. G., Conen, F., Griffith, A. D., Reimann, S., Steinbacher, M., Krummel, P. B., Steele, L. P., van der Schoot, M. V., Galbally, I. E., Molloy, S. B., and Barnes, J. E.: Towards a universal "baseline" characterisation of air masses for high- and low-altitude observing stations using radon-222, Aerosol Air Qual. Res., 16, 885–899, https://doi.org/10.4209/aaqr.2015.06.0391, 2016.

Chen, J., Wu, Z., Chen, J., Reicher, N., Fang, X., Rudich, Y., and Hu, M.: Size-resolved atmospheric ice-nucleating particles during East Asian dust events, Atmos. Chem. Phys., 21, 3491–3506, https://doi.org/10.5194/acp-21-3491-2021, 2021.

Collaud Coen, M., Weingartner, E., Schaub, D., Hueglin, C., Corrigan, C., Henning, S., Schwikowski, M., and Baltensperger, U.: Saharan dust events at the Jungfraujoch: detection by wavelength dependence of the single scattering albedo and first climatology analysis, Atmos. Chem. Phys., 4, 2465–2480, https://doi.org/10.5194/acp-4-2465-2004, 2004.

Collaud Coen, M., Weingartner, E., Furger, M., Nyeki, S., Prévôt, A. S. H., Steinbacher, M., and Baltensperger, U.: Aerosol climatology and planetary boundary influence at the Jungfraujoch analyzed by synoptic weather types, Atmos. Chem. Phys., 11, 5931–5944, https://doi.org/10.5194/acp-11-5931-2011, 2011.

Conen, F., Morris, C. E., Leifeld, J., Yakutin, M. V., and Alewell, C.: Biological residues define the ice nucleation properties of soil dust, Atmos. Chem. Phys., 11, 9643–9648, https://doi.org/10.5194/acp-11-9643-2011, 2011.

Conen, F., Henne, S., Morris, C. E., and Alewell, C.: Atmospheric ice nucleators active ≥ −12 °C can be quantified on $PM_{10}$ filters, Atmos. Meas. Tech., 5, 321–327, https://doi.org/10.5194/amt-5-321-2012, 2012.

Conen, F., Rodríguez, S., Hülin, C., Henne, S., Herrmann, E., Bukowiecki, N., and Alewell, C.: Atmospheric ice nuclei at the high-altitude observatory Jungfraujoch, Switzerland, Tellus B, 67, 25014, https://doi.org/10.3402/tellusb.v67.25014, 2015.

Conen, F., Yakutin, M. V., Yttri, K. E., and Hüglin, C.: Ice nucleating particle concentrations increase when leaves fall in autumn, Atmosphere, 8, 202, https://doi.org/10.3390/atmos8100202, 2017.

Conen, F. and Yakutin, M. V.: Soils rich in biological ice-nucleating particles abound in ice-nucleating macromolecules likely produced by fungi, Biogeosciences, 15, 4381–4385, https://doi.org/10.5194/bg-15-4381-2018, 2018.

Conen, F. and Zimmermann, L.: Separating "free tropospheric conditions" from those "influenced by the planetary boundary layer", International Foundation HFSJG Activity Report 2020, 49–50, https://www.hfsjg.ch/reports/2020/pdf/120_UniBasel_Conen_radon_cf.pdf, last access: 2 August 2021.

Daily, M. I., Tarn, M. D., Whale, T. F., and Murray, B. J.: The sensitivity of the ice-nucleating ability of minerals to heat and the implications for the heat test for biological ice nucleators, Atmos. Meas. Tech. Discuss. [preprint], https://doi.org/10.5194/amt-2021-208, in review, 2021.

DeMott, P. J., Prenni, A. J., Liu, X., Kreidenweis, S. M., Petters, M. D., Twohy, C. H., Richardson, M. S., Eidhammer, T., and Rogers, D. C.: Predicting global atmospheric ice nuclei distributions and their impacts on climate, P. Natl. Acad. Sci. USA, 107, 11217–11222, https://doi.org/10.1073/pnas.0910818107, 2010.

Diehl, K., Matthias-Maser, S., Jaenicke, R., and Mitra, S. K.: The ice nucleation ability of pollen Part II: Laboratory studies in immersion and contact freezing modes, Atmos. Res., 61, 125–133, 2002.

Failor, K. C., Schmale III, D. G., Vinatzer, B. A., and Monteil, C. L.: Ice nucleation active bacteria in precipitation are genetically diverse and nucleate ice by employing different mechanisms, ISME J., 11, 2740–2753, https://doi.org/10.1038/ismej.2017.124, 2017.

Findeisen, W.: Die kolloidmeteorologischen Vorgänge bei der Niederschlagsbildung (Colloidal meteorological processes in the formation of precipitation), Meteorol. Z., 55, 121–133, 1938.

Fröhlich-Nowoisky, J., Hill, T. C. J., Pummer, B. G., Yordanova, P., Franc, G. D., and Pöschl, U.: Ice nucleation activity in the widespread soil fungus *Mortierella alpina*, Biogeosciences, 12, 1057–1071, https://doi.org/10.5194/bg-12-1057-2015, 2015.

Fukuta, N. and Takahashi, T.: The growth of atmospheric ice crystals: A summary of findings in vertical supercooled cloud tunnel studies, J. Atmos. Sci., 56, 1963–1979, 1999.

Griffiths, A. D., Conen, F., Weingartner, E., Zimmermann, L., Chambers, S. D., Williams, A. G., and Steinbacher, M.: Surface-to-mountaintop transport characterised by radon observations at the Jungfraujoch, Atmos. Chem. Phys., 14, 12763–12779, https://doi.org/10.5194/acp-14-12763-2014, 2014.

Hammer, E., Bukowiecki, N., Gysel, M., Jurányi, Z., Hoyle, C. R., Vogt, R., Baltensperger, U., and Weingartner, E.: Investigation of the effective peak supersaturation for liquid-phase clouds at the high-alpine site Jungfraujoch, Switzerland (3580 m a.s.l.), Atmos. Chem. Phys., 14, 1123–1139, https://doi.org/10.5194/acp-14-1123-2014, 2014.

Harrison, A. D., Lever, K., Sanchez-Marroquin, A., Holden, M. A., Whale, T. F., Tarn, M. D., McQuaid, J. B., and Murray, B. J.: The ice-nucleating ability of quartz immersed in water and its atmospheric importance compared to K-feldspar, Atmos. Chem. Phys., 19, 11343–11361, https://doi.org/10.5194/acp-19-11343-2019, 2019.

He, C., Yin, Y., Wang, W., Chen, K., Mai, R., Jiang, H., Zhang, X., and Fang, C.: Aircraft observations of ice nucleating particles over the Northern China Plain: Two cases studies, Atmos. Res., 248, 105242, https://doi.org/10.1016/j.atmosres.2020.105242, 2021.

Henne, S., Furer, M., and Prévòt, A. S. H.: Climatology of mountain venting-induced elevated moisture layers in the lee of the Alps, J. Appl. Meteorol., 44, 620-633, https://doi.org/10.1175/JAM2217.1, 2005.

Herrmann, E., Weingartner, E., Henne, S., Vuilleumier, L., Bukowiecki, N., Steinbacher, M., Conen, F., Coen, M. C., Hammer, E., Jurányi, Z., Baltensperger, U., and Gysel, M.: Analysis of long-term aerosol size distribution data from Jungfraujoch with emphasis on free tropospheric conditions, cloud influence, and air mass transport, J. Geophys. Res., 120, 9459–9480, https://doi.org/10.1002/2015JD023660, 2015.

Hill, T. C. J., DeMott, P. J., Tobo, Y., Fröhlich-Nowoisky, J., Moffett, B. F., Franc, G. D., and Kreidenweis, S. M.: Sources of organic ice nucleating particles in soils, Atmos. Chem. Phys., 16, 7195–7211, https://doi.org/10.5194/acp-16-7195-2016, 2016.

Hirano, S. S. and Upper, C. D.: Bacteria in the Leaf Ecosystem with Emphasis on Pseudomonas syringae – a Pathogen, Ice Nucleus, and Epiphyte, Microbiol. Mol. Biol. Rev., 64, 624–653, 2000.

Huffman, J. A., Prenni, A. J., DeMott, P. J., Pöhlker, C., Mason, R. H., Robinson, N. H., Fröhlich-Nowoisky, J., Tobo, Y., Després, V. R., Garcia, E., Gochis, D. J., Harris, E., Müller-Germann, I., Ruzene, C., Schmer, B., Sinha, B., Day, D. A., Andreae, M. O., Jimenez, J. L., Gallagher, M., Kreidenweis, S. M., Bertram, A. K., and Pöschl, U.: High concentrations of biological aerosol particles and ice nuclei during and after rain, Atmos. Chem. Phys., 13, 6151–6164, https://doi.org/10.5194/acp-13-6151-2013, 2013.

Iwata, A., Imura, M., Hama, M., Maki, T., Tsuchiya, N., Kunihisa, R., and Matsuki, A.: Release of Highly Active Ice Nucleating Biological Particles Associated with Rain, Atmosphere, 10, 605, https://doi.org/10.3390/atmos10100605, 2019.

Kanitz, T., Seifert, P., Ansmann, A., Engelmann, R., Althausen, D., Casiccia, C., and Rohwer, E. G.: Contrasting the impact of aerosols at northern and southern midlatitudes on heterogeneous ice formation, Geophys. Res. Lett., 38, L17802, https://doi.org/10.1029/2011GL048532, 2011.

Keller, M. D., Bergstrom, G. C., and Shields, E. J.: The aerobiology of Fusarium graminearum, Aerobiologia, 30, 123–136, https://doi.org/10.1007/s10453-013-9321-3, 2014.

Kiefft, T. L.: Ice nucleation activity in lichens, Appl. Environ. Microbiol., 54, 1678–1681, 1988.

Kunert, A. T., Pöhlker, M. L., Tang, K., Krevert, C. S., Wieder, C., Speth, K. R., Hanson, L. E., Morris, C. E., Schmale III, D. G., Pöschl, U., and Fröhlich-Nowoisky, J.: Macromolecular fungal ice nuclei in *Fusarium*: effects of physical and chemical processing, Biogeosciences, 16, 4647–4659, https://doi.org/10.5194/bg-16-4647-2019, 2019.

Lacher, L., DeMott, P. J., Levin, E. J. T., Suski, K. J., Boose, Y., Zipori, A., Herrmann, E., Bukowiecki, N., Steinbacher, M., Gute, E., Abbatt, J. P., Lohmann, U., and Kanji, Z. A.: Background free-tropospheric ice nucleating particle concentrations at mixed-phase cloud conditions, J. Geophys. Res.-Atmos., 123, 10506–10525, https://doi.org/10.1029/2018JD028338, 2018.

Lacher, L., Clemen, H.-C., Shen, X., Mertes, S., Gysel-Beer, M., Moallemi, A., Steinbacher, M., Henne, S., Saathoff, H., Möhler, O., Höhler, K., Schiebel, T., Weber, D., Schrod, J., Schneider, J., and Kanji, Z. A.: Sources and nature of ice-nucleating particles in the free troposphere at Jungfraujoch in winter 2017, Atmos. Chem. Phys., 21, 16925–16953, https://doi.org/10.5194/acp-21-16925-2021, 2021.

Limpert, E., Stahel, W. A., and Abbt, M.: Log-normal distributions across the sciences: Keys and clues, BioScience, 51, 341–352, http://stat.ethz.ch/~stahel/lognormal/bioscience.pdf (last access: 2 August 2021), 2001.

Limpert, E., Burke, J., Galan, C., del Mar Trigo, M., West, J. S., and Stahel, W. A.: Data, not only in aerobiology: How normal is the normal distribution? Aerobiologia 2008, 24, 121–124, https://doi.org/10.1007/s10453-008-9092-4, 2008.

Lindemann, J., Constantinidou, H. A., Barchet, W. R., and Upper, C. D.: Plants as sources of airborne bacteria, including ice nucleation-active bacteria, Appl. Environ. Microbiol., 44, 1059–1063, 1982.

Lindow, S. E., Arny, D. C., and Upper, C. D.: Distribution of ice nucleation-active bacteria on plants in nature, Appl. Environ. Microbiol., 36, 831–838, 1978.

McCluskey, C. S., Ovadnevaite, J., Rinaldi, M., Atkinson, J., Belosi, F., Ceburnis, D., Marullo, S., Hill, T. C. J., Lohmann, U., Kanji, Z. A., O'Dowd, C., Kreidenweis, S. M., and DeMott, P. J..: Marine and terrestrial organic ice-nucleating particles in pristine marine to continentally influenced northeast Atlantic air masses, J. Geophys. Res.-Atmos. 123, 6196–6212, https://doi.org/10.1029/2017JD028033, 2018.

Mertes, S., Verheggen, B., Walter, S., Connolly, P., Ebert, M., Schneider, J., Bower, K. N., Cozic, J., Weinbruch, S., Baltensperger, U., and Weingartner, E.: Counterflow virtual impactor based collection of small ice particles in mixed-phase clouds for the physico-chemical characterization of tropospheric ice nuclei: sampler description and first case study, Aerosol Sci. Tech., 41, 848–864, https://doi.org/10.1080/02786820701501881, 2007.

Mignani, C., Wieder, J., Sprenger, M. A., Kanji, Z. A., Henneberger, J., Alewell, C., and Conen, F.: Towards parameterising atmospheric concentrations of ice-nucleating particles active at moderate supercooling, Atmos. Chem. Phys., 21, 657–664, https://doi.org/10.5194/acp-21-657-2021, 2021.

Morris, C. E., Sands, D. C., Glaux, C., Samsatly, J., Asaad, S., Moukahel, A. R., Gonçalves, F. L. T., and Bigg, E. K.: Urediospores of rust fungi are ice nucleation active at > −10 °C and harbor ice nucleation active bacteria, Atmos. Chem. Phys., 13, 4223–4233, https://doi.org/10.5194/acp-13-4223-2013, 2013.

O'Sullivan, D., Murray, B. J., Ross, J. F., Whale, T. F., Price, H. C., Atkinson, J. D., Umo, N. S., and Webb, M. E.: The relevance of nanoscale biological fragments for ice nucleation in clouds, Sci. Rep., 5, 8082, https://doi.org/10.1038/srep08082, 2015.

Patade, S., Phillips, V. T. J., Amato, P., Bingemer, H. G., Burrows, S. M., DeMott, P. J., Goncalves, F. L. T., Knopf, D. A., Morris, C. E., Alwmark, C., Artaxo, P., Pöhlker, C., Schrod, J., and Weber, B.: Empirical formulation for multiple groups of primary biological ice nucleating particles from field observations over Amazonia, J. Atmos. Sci, 78, 2195–2220, https://doi.org/10.1175/JAS-D-20-0096.1, 2021.

Perkins, R. J., Gillette, S. M., Hill, T. C. J., and DeMott, P. J.: The Labile Nature of Ice Nucleation by Arizona Test Dust, ACS. Earth. Space. Chem., 4, 133–141, https://doi.org/10.1021/acsearthspacechem.9b00304, 2020.

Petters, M. D. and Wright, T. P.: Revisiting ice nucleation from precipitation samples, Geophys. Res. Lett., 42, 8758–8766, https://doi.org/10.1002/2015GL065733, 2015.

Phelps, P., Giddings, T. H., Prochoda, M., and Fall, R.: Release of cell-free ice nuclei by Erwinia herbicola, J. Bacteriol., 167, 496–502, 1986.

Polen, M., Lawlis, E., and Sullivan, R. C.: The unstable ice nucleation properties of Snomax® bacterial particles, J. Geophys. Res. Atmos., 121, 11666–11678, https://doi.org/10.1002/2016JD025251, 2016.

Pouleur, S., Richard, C., Martin, J.-G., and Antoun, H.: Ice nucleation activity in Fusarium acuminatum and Fusarium avenaceum, Appl. Environ. Microbiol., 58, 2960–2964, 1992.

Prenni, A.J., Tobo, Y., Garcia, E., DeMott, P.J., Huffman, J.A., McCluskey, C.S., Kreidenweis, S.M., Prenni, J., Pöhlker, C., Pöschl, U.: The impact of rain on ice nuclei populations at a forested site in Colorado, Geophys. Res. Lett., 40, 227–231, https://doi.org/10.1029/2012GL053953, 2013.

Pummer, B. G., Bauer, H., Bernardi, J., Bleicher, S., and Grothe, H.: Suspendable macromolecules are responsible for ice nucleation activity of birch and conifer pollen, Atmos. Chem. Phys., 12, 2541–2550, https://doi.org/10.5194/acp-12-2541-2012, 2012.

Schmidt, S., Schneider, J., Klimach, T., Mertes, S., Schenk, L. P., Kupiszewski, P., Curtius, J., and Borrmann, S.: Online single particle analysis of ice particle residuals from mountain-top mixed-phase clouds using laboratory derived particle type assignment, Atmos. Chem. Phys., 17, 575–594, https://doi.org/10.5194/acp-17-575-2017, 2017.

Schnell, R. C. and Vali, G.: Worldwide souce of leaf derived freezing nuclei, Nature, 246, 212–213, 1973.

Schwikowski, M., Seibert, P., Baltensperger, U., and Gäggeler, H. W.: A study of an outstanding Saharan dust event at the high-alpine site Jungfraujoch, Switzerland, Atmos. Environ., 29, 1829–1842, https://doi.org/10.1016/1352-2310(95)00060-C, 1995.

Sun, J., Herrmann, M., Yuan, Y., Birmili, W., Collaud Coen, M., Weinhold, K., Madueno, L., Poulain, L., Tuch, T., Ries, L., Sohmer, R., Couret, C., Frank, G., Brem, B. T., Gysel-Beer, M., Ma, N., and Wiedensohler, A.: Long-term trends of black carbon and particle number concentration in the lower free troposphere in Central Europe, Environ. Sci. Eur., 33, 47, https://doi.org/10.1186/s12302-021-00488-w, 2021.

Suski, K. J., Hill, T. C. J., Levin, E. J. T., Miller, A., DeMott, P. J., and Kreidenweis, S. M.: Agricultural harvesting emissions of ice-nucleating particles, Atmos. Chem. Phys., 18, 13755–13771, https://doi.org/10.5194/acp-18-13755-2018, 2018.

Testa, B., Hill, T. C. J., Marsden, N., Barry, K. R., Hume, C. C., Bian, Q., Uetake, J., Hare, H., Perkins, J. R., Möhler, O., Kreidenweis, S. M., and DeMott, P. J.: Ice nucleating particle connections to regional Argentinian land surface emissions and weather during the Cloud, Aerosol, and Complex Terrain Interactions experiment, J. Geophys. Res Atmos., 126, e2021JD035186, https://doi.org/10.1029/2021JD035186, 2021.

Tignat-Perrier, R., Dommergue, A., Thollot, A., Keuschnig, C., Magand, O., Vogel, T. M., and Larose, C.: Global airborne microbial communities controlled by landscapes and wind condition, Sci. Rep., 9, 14441, https://doi.org/10.1038/s41598-019-51073-4, 2019.

Vali, G.: Quantitative evaluation of experimental results on the heterogeneous freezing nucleation of supercooled liquids, J. Atmos. Sci., 28, 402–409, https://doi.org/10.1175/1520-0469(1971)028<0402:QEOERA>2.0.CO;2, 1971.

Vali, G.: Repeatability and randomness in heterogeneous freezing nucleation, Atmos. Chem. Phys., 8, 5017–5031, https://doi.org/10.5194/acp-8-5017-2008, 2008.

Vergara-Temprado, J., Murray, B. J., Wilson, T. W., O'Sullivan, D., Browse, J., Pringle, K. J., Ardon-Dryer, K., Bertram, A. K., Burrows, S. M., Ceburnis, D., DeMott, P. J., Mason, R. H., O'Dowd, C. D., Rinaldi, M., and Carslaw, K. S.: Contribution of feldspar and marine organic aerosols to global ice nucleating particle concentrations, Atmos. Chem. Phys., 17, 3637–3658, https://doi.org/10.5194/acp-17-3637-2017, 2017.

Vasebi, Y., Mechan Llontop, M. E., Hanlon, R., Schmale III, D. G., Schnell, R., and Vinatzer, B. A.: Comprehensive characterization of an aspen (*Populus tremuloides*) leaf litter sample that maintained ice nucleation activity for 48 years, Biogeosciences, 16, 1675–1683, https://doi.org/10.5194/bg-16-1675-2019, 2019.

Vujanovic, V., Goh, Y. K., and Daida, P.: Heat- and Cold-Shock Responses in Fusarium graminearum 3 Acetyl- and 15 Acetyl-Deoxynivalenol Chemotypes, J. Microbiol., 50, 97–102, https://doi.org/10.1007/s12275-012-1381-5, 2012.

Weingartner, E., Nyeki, S., and Baltensperger, U.: Seasonal and diurnal variation of aerosol size distributions ($10 < D < 750$ nm) at a high-alpine site (Jungfraujoch 3580 m a.s.l.), J. Geophys. Res., 104, 26809–26820, https://doi.org/10.1029/1999JD900170, 1999.

Wieder, J., Mignani, C., Schär, M., Roth, L., Sprenger, M., Henneberger, J., Lohmann, U., Brunner, C., and Kanji, Z. A.: Unveiling atmospheric transport and mixing mechanisms of ice nucleating particles over the Alps, Atmos. Chem. Phys. Discuss. [preprint], https://doi.org/10.5194/acp-2021-718, in review, 2021.

Whittlestone, S. and Zahorowski, W.: Baselineradon detectors for shipboard use: Development and deployment in the First Aerosol Characterization Experiment (ACE 1), J. Geophys. Res., 103, 16743–16751, 1998.